little concentrated HNO_3, the solution is then evaporated to dryness and dissolved in 10 ml 25% HCl at 60°C. About 5 ml of a 25% K_2SO_3 solution are added to reduce the oxide. The tellurium is centrifuged and dried. It is then weighed into a small quartz tube with an equivalent amount of pure zinc. The tube is evacuated, sealed off and placed in an oven that is brought to 700°C, at which temperature ZnTe is rapidly formed by a vapor-phase reaction. The tube is opened after it has cooled slowly. The brick-red zinc telluride is usually scraped off the wall of the tube under some toluene. This requires some care, but it can be done almost quantitatively.

ACKNOWLEDGMENTS

The authors wish to thank S. A. Drentje for performing the mass separation of the Te isotopes.

This investigation is partly supported by the Foundation for Fundamental Research on Matter (F.O.M.) subsidized by the Netherlands Organization for Pure Scientific Research (Z.W.O.).

PHYSICAL REVIEW VOLUME 146, NUMBER 3 17 JUNE 1966

$W^{182}(d,p)W^{183}$ Reaction at 7.5 and 12 MeV: An Investigation of the Stripping Process on a Deformed Heavy Nucleus*

R. H. Siemssen and J. R. Erskine
Argonne National Laboratory, Argonne, Illinois
(Received 24 January 1966)

The $W^{182}(d,p)W^{183}$ reaction has been studied at 7.5 and at 12 MeV with a broad-range magnetic spectrograph. At 12 MeV, angular distributions have been obtained from 5° to 145° for the transitions to the ground state and to the levels at excitations of 46, 99, 208, 292, 412, and 453 keV. In addition, the scattering of deuterons on W^{182} and protons on W^{183} has been measured at 12 MeV. The elastic scattering has been analyzed in terms of the nuclear optical model. A serious ambiguity in the deuteron parameters has been observed. For inelastic deuteron scattering leaving W^{182} in its first excited state, a distorted-wave Born-approximation (DWBA) analysis based on a deformed complex potential leads to a deformation parameter $\beta=0.23$ for W^{182}. The angular distributions of the $W^{182}(d,p)W^{183}$ reaction have been compared with DWBA calculations with different distorting potentials, and spectroscopic factors have been extracted. The ratios of the experimental spectroscopic factors agree quite well with those predicted by the Nilsson model, when band mixing is included in the calculation of the theoretical spectroscopic factors. Absolute spectroscopic factors, on the other hand, may disagree by as much as a factor of 2–3. The data have also been compared with the DWBA calculations of Penny and Satchler, which include "two-step" processes. Our results indicate that "two-step" processes are probably unimportant for the reaction studied.

I. INTRODUCTION

THE investigation of deformed heavy nuclei by means of charged-particle reactions [in particular with (d,p) and (d,t) reactions] has only recently become possible through the use of the tandem Van de Graaff accelerator in combination with magnetic spectrographs. So far only a few angular distributions have been published,[1–4] and none of these have been compared with the predictions of the distorted-wave Born approximation (DWBA) theory utilizing measured distortion parameters. In view of the large static deformation of the rare-earth and the actinide nuclei, such a test of the DWBA theory seems of interest, since one might expect inelastic-scattering (strong coupling) effects[5,6] to be significant. In particular, it is desirable to investigate how accurately spectroscopic information can be obtained from (d,p) and (d,t) reactions on these nuclei.

For our investigation, we have chosen the W^{182}-$(d,p)W^{183}$ reaction. The energy-level scheme of W^{183} (up to approximately 500 keV) has been extensively studied.[7,8] The levels (Fig. 1) which we observe in the (d,p) reaction are the $[510]\frac{1}{2}^-$, $[512]\frac{3}{2}^-$, and $[503]\frac{7}{2}^-$ intrinsic states[9] and the various rotational levels built

* Work performed under the auspices of the U. S. Atomic Energy Commission.

[1] M. N. Vergnes and R. K. Sheline, Phys. Rev. **132**, 1736 (1963).
[2] A. Isoya, Phys. Rev. **130**, 234 (1963).
[3] J. R. Erskine and W. W. Buechner, Phys. Rev. **133**, B370 (1964).
[4] B. E. F. Macefield and R. Middleton, Nucl. Phys. **59**, 561 (1964).
[5] S. K. Penny and G. R. Satchler, Nucl. Phys. **53**, 145 (1964).
[6] P. Iano and N. Anstern Bull. Am. Phys. Soc. **11**, 665 (1964); P. Iano, thesis, University of Pittsburgh, 1965 (unpublished).
[7] J. J. Murray, F. Boehm, P. Marmier, and J. W. M. Du Mond, Phys. Rev. **97**, 1007 (1955); C. J. Gallagher, Jr., and H. L. Nielsen, Nucl. Phys. **24**, 422 (1961); B. Harmatz, T. H. Handley, and J. W. Mihelich, Phys. Rev. **128**, 1186 (1962); W. F. Edwards, F. Boehm, J. Rogers, and E. J. Seppi, Nucl. Phys. **63**, 97 (1965).
[8] J. R. Erskine, Phys. Rev. **138**, B66 (1965).
[9] The intrinsic states are labeled with the asymptotic quantum numbers $(Nn_z\Lambda\Omega\pi)$, where N is the total oscillator quantum number, n_z is the number of oscillator quanta along the symmetry axis, Λ is the component of the total orbital angular momentum along the symmetry axis, and Ω is the component of total angular momentum along the symmetry axis.

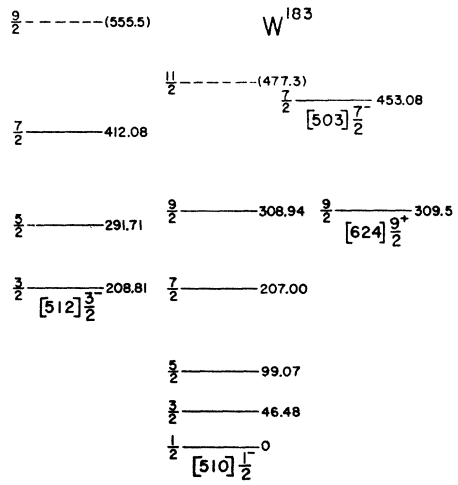

FIG. 1. The level scheme of W^{183}. The energies and the spin and parity assignments have been taken from Ref. 7.

upon these states. These have been well identified by previous[7,8] investigations. Consequently, it is possible to calculate the spectroscopic factors involved in the $W^{182}(d,p)W^{183}$ reaction with a fair degree of certainty. The $W^{182}(d,p)W^{183}$ reaction can therefore be expected to provide a sensitive test of the accuracy of the DWBA theory.

Angular distributions of the (d,p) reaction have been measured at $E_d=12.0$ MeV because this is the average maximum bombarding energy of the first generation of tandem Van de Graaffs and also at 7.5 MeV because at this energy the distortions are dominated by the Coulomb field. (The Coulomb barrier of W^{182} for deuterons and protons is about 12 MeV.) Therefore, the ambiguities in the nuclear part of the optical potentials will probably reflect themselves less seriously[10–12] in the extraction of the spectroscopic factors. A spectroscopic study of the $W^{182}(d,p)W^{183}$ reaction has been previously published[8] by one of us (JRE).

In order to obtain the distorting potentials for the DWBA analysis of the (d,p) data, we have in addition measured the scattering of 12-MeV deuterons from W^{182} and protons from W^{183}. Since the analysis of the scattering of deuterons in terms of the nuclear optical model in the rare-earth mass region[13] has as so far been based on data which did not separate the elastic from the inelastic deuteron scattering, our high-resolution measurement of the deuteron scattering was desirable. Thus as a by-product we have obtained an angular distribution of the inelastically scattered deuterons leading to the 2^+ level of the ground-state rotational band. In the proton scattering experiment, it was not possible to separate the inelastic groups from the elastic group. However, a strong-coupling calculation[14] indicates that the contribution of the inelastic proton scattering to the unseparated scattering cross section is less important than in the deuteron-scattering experiment.

II. EXPERIMENTAL PROCEDURE AND RESULTS

The 7.5-MeV data were taken with the multiple-gap magnetic spectrograph[15] at the Massachusetts Institute of Technology. One bombardment of about 5000 μC was made with nuclear-track plates loaded in all gaps from 90° to 172½°. Aluminum foil was used in front of each plate holder to prevent elastically scattered deuterons from reaching the emulsions. For the determination of the absolute differential cross section, data were taken at Argonne National Laboratory with a single-gap magnetic spectrograph.[16] The absolute differential cross section of the $W^{182}(d,p)W^{183}$ reaction was measured at 142½° and a bombarding energy of 7.5 MeV. The data were normalized to the deuteron elastic-scattering cross section. At 7.5 MeV, the latter is nearly pure Coulomb scattering, as was confirmed by an optical-model calculation with reasonable distortion parameters.

The measurements at 12 MeV have been made with the Argonne tandem Van de Graaff and broad-range magnetic spectrograph. This spectrograph has already been described elsewhere.[16] Nuclear track plates were

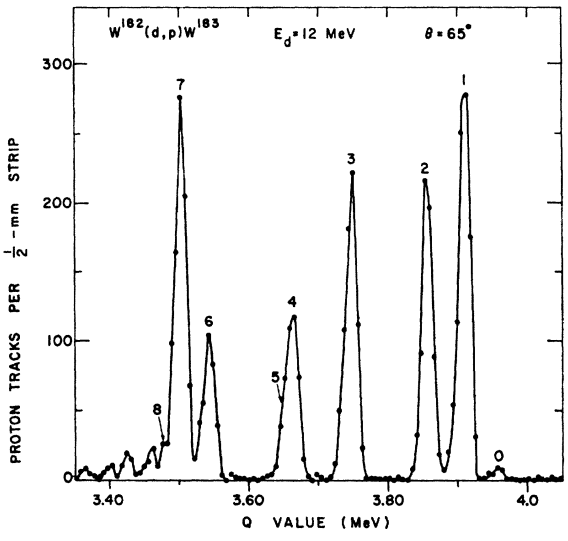

FIG. 2. Proton spectrum from the $W^{182}(d,p)W^{183}$ reaction at $E_d=12$ MeV as observed with the broad-range magnetic spectrograph.

[10] A. K. Kerman and F. P. Gibson, in Argonne National Laboratory Report ANL-6848, edited by F. E. Throw, p. 43 (unpublished); Bull. Am. Phys. Soc. 9, 675 (1964).
[11] L. J. B. Goldfarb, Nucl. Phys. 72, 537 (1965).
[12] W. R. Smith, Nucl. Phys. 72, 593 (1965).
[13] C. M. Perey and F. G. Perey, Phys. Rev. 132, 755 (1963).
[14] The calculations were performed with the strong-coupling code ROTS by R. C. Barrett, Nucl. Phys. 51, 27 (1964).
[15] H. A. Engle and W. W. Buechner, Rev. Sci. Instr. 34, 155 (1963).
[16] J. R. Erskine, Phys. Rev. 135, B110 (1964).

used to record the analyzed particles. Absorber foils were inserted in front of the plates to eliminate all but the proton tracks. Typical exposures ranged from 2000 to 5000 μC. A spectrum is shown in Fig. 2. A solid-state detector at a scattering angle of 90° was used as a monitor. The number of deuterons elastically scattered from W^{182} and recorded during each exposure was used to normalize the various runs.

The elastic-scattering data were taken with a solid-state detector in an 18-in. scattering chamber. Inelastically and elastically scattered deuterons were also recorded with the magnetic spectrograph at the same time that the (d,p) exposures were made. Spectrograph and counter data agree within the experimental errors. Absolute differential cross sections for elastic scattering were determined within an uncertainty of 5% from measurements at a scattering angle of 60° by comparing the yields at 12 MeV with those at 5 MeV where the scattering is assumed to be purely Rutherford. A magnetic-spectrograph plate exposed briefly to the elastically scattered deuterons was used to normalize the reaction data to the scattering data at 110°. The error in the absolute differential cross section for the reaction data is estimated to be $\leqslant 10\%$.

Targets were made from separated isotopes of W^{182} and W^{183} by evaporating WO_3 onto thin self-supporting backings of carbon with a Formvar substrate. Target thicknesses ranged from 50 to 100 $\mu g/cm^2$. The isotopes W^{182} and W^{183} (obtained from Oak Ridge National Laboratory) were enriched to 94% and 83%, respectively.

The proton and deuteron scattering data are shown in Figs. 3 and 5 together with the theoretical curves obtained from the optical-model analysis of the data which will be discussed below. The angular distribution of the inelastically scattered deuterons is presented in Fig. 6. The cross sections for elastic and inelastic scattering are listed in Tables I and II. Angular distributions have been obtained for approximately twenty proton groups from the $W^{182}(d,p)W^{183}$ reaction. Since this paper is mainly concerned with the reaction mechanism, the present analysis included only the transitions to the levels up to 453-keV excitation for which the spectroscopic data are known[7,8] from other measurements. The measured angular distributions of proton groups leading to the ground state, and the 46-, 99-, 209-, 292-, 412-, and 453-keV states in W^{183} are given in Figs. 7–10 of Secs. IIIA and IIIB and also in Table III. The angular distributions taken at $E_d=7.5$ MeV are shown in Fig. 11 (Sec. IIIB) for transitions to the 45- and 99-keV states. The curves through the data points are DWBA calculations which will be discussed below. Error bars shown in the figures are the statistical errors only.

In the analysis of the spectrograph data, care was taken that none of the proton groups of interest were confused with weak contaminant groups that were present. At the far forward angles, where the yield in the $W^{182}(d,p)W^{183}$ reaction is very low, the possibility of some contamination of the data cannot be ruled out.

TABLE I. Elastic-scattering cross sections for the $W^{183}(p,p)W^{183}$ reaction at 12 MeV. The estimated total error in the cross section is $\leqslant 5\%$.

$\theta_{c.m.}$ (degrees)	σ (mb/sr)
35.2	5840
40.2	3520
45.2	2180
50.2	1490
55.3	1010
60.3	729
65.3	512
70.3	369
75.3	260
80.3	200
85.3	163
90.3	136
95.3	111
100.3	94.2
105.3	79.8
110.3	65.0
115.3	54.2
120.3	47.2
125.3	40.9
130.2	37.4
135.2	34.6
140.2	30.2
145.2	28.6
150.2	27.1
155.1	26.1

TABLE II. Cross sections for the elastic and the inelastic scattering of deuterons on W^{182} at 12 MeV. The estimated total error in the cross section is $\leqslant 5\%$.

$\theta_{c.m.}$ (degrees)	$\sigma_{elastic}$ (mb/sr)	$\sigma_{inelastic}$ (mb/sr)
20.2	54800	
25.3	22300	
30.3	11300	
35.4	6410	
40.4	3620	
45.4	2190	
50.5	1370	6.45±0.09
55.5	873	
60.5	611	4.98±0.07
65.5	412	
70.6	293	5.52±0.08
75.6	205	5.26±0.37
80.6	152	5.50±0.08
85.6	110	5.10±0.35
90.6	87.5	4.64±0.07
95.6	70.2	4.78±0.20
100.6	54.2	4.07±0.07
105.6	46.0	3.91±0.19
110.6	37.0	3.53±0.10
115.6	30.9	2.67±0.14
120.6	26.0	2.83±0.08
125.5	21.9	2.84±0.12
130.5	19.3	2.66±0.03
135.4	17.0	2.32±0.10
140.4	14.6	2.59±0.09
145.4	13.5	2.43±0.03
150.3	12.3	2.54±0.09
155.3	11.6	2.44±0.07
160.2	10.7	2.37±0.07

TABLE III. Absolute differential cross sections (mb/sr) for the $W^{182}(d,p)W^{183}$ reaction at $E_d=12$ MeV. The errors do not include the error in the absolute cross section, which is believed to be $\leqslant 10\%$.

	Absolute differential cross section (mb/sr)						
$\theta_{c.m.}$ (degrees)	At $E_x=0$	At $E_x=46$ keV	At $E_x=99$ keV	At $E_x=207$ keV, $E_x=209$ keV	At $E_x=292$ keV, $E_x=309$ keV	At $E_x=412$ keV	At $E_x=453$ keV
5.0		106± 6	47± 4	79± 6	57± 5	38± 8	135±13
10.1	14 ±2	193±10	31± 7	126± 7	45± 4	45± 8	147±15
15.1	22 ±4	227± 7	37± 3	149± 8	38± 4	33± 4	106± 7
20.1	16 ±2	271±13	44± 7	200±12	56± 4	21± 5	89±14
25.2		291±10	84± 5	196± 8	73± 5	25± 3	112± 6
30.2	14 ±6	283±17	136±15	206± 8	90±10	46± 7	170±13
35.2	29 ±6	386±11	184± 8	235± 9	126± 6	63± 5	235± 9
40.2		510±28	257±18	261±15	150±12	108±10	343±18
50.3	24 ±6	516±18	291±14	336±15	185±11	121± 9	344±15
60.3	11 ±3	402±20	276±17	314±18	175±14	136±12	350±21
65.4	11 ±2	378±13	269±11	291±11	181± 9	136± 8	343±12
70.4	16 ±4	416±21	235±16	302±18	169±13	137±12	372±47
80.4	26 ±6	373±20	262±17	219±15	190±14	134±12	342±36
85.4	11 ±2	339±12	235±10	206± 9	159± 8	135± 8	349±12
90.4		259±16	218±15	187±14	183±14	134±12	338±31
100.4		195±14	206±14	165±13	132±11	123±11	330±36
105.4	5.3±1.3	144± 7	174± 8	148± 7	127± 7		259± 9
110.4		155±12	142± 7	136±12	123±11	90± 9	244±33
125.3	4.8±1.3	135± 7	124± 7	101± 6	101± 6	81± 5	206± 8
130.3		111± 6	115± 6	86± 5	97± 5	61± 5	210±16
145.2	4.7±1.2	91± 5	95± 6	70± 5	85± 5	62± 4	172±10

although we feel quite confident that the data presented are clean.

III. DISCUSSION

A. Analysis of the Scattering Data

The elastic-scattering data were analyzed in terms of the nuclear optical model by means of the search code JIB3 by Perey.[17] In the calculation, the potentials were taken to be of the standard Woods-Saxon type with a surface absorption, as defined by the expression

$$U(r)=V_c(r)-Vf(r,r_0,a)+4ia_IW(d/dr)f(r,r_{0I},a_I)+(\hbar/m_\pi c)^2V_{LS}(1/r)(d/dr)f(r,r_0,a), \quad (1)$$

with

$$f(r,r_0,a)=1+\exp[(r-r_0A^{1/3})/a]^{-1}.$$

Here V_c is the Coulomb potential, V and W are the real and imaginary parts of the central potential, and V_{LS} is the spin-orbit potential. Spin-orbit coupling was taken into account in the analysis of the proton-scattering data but not the deuteron-scattering data. The strength used for the spin-orbit potential was $V_{LS}=7.5$ MeV.

A search only on V and W already gave a satisfactory fit to our proton scattering data (Fig. 3) if the geometrical parameters (r_0,r_{0I},a,a_I) were chosen to be the same as the average parameters that Perey[18] found from the analysis of proton scattering from heavy nuclei. The real potential, V found from the search calculation is approximately 2 MeV shallower than Perey's "average" potential calculated from Eq. (2) in Ref. 19. If, in addition, the search is extended to include the diffuseness (a and a_I) of the real and imaginary wells, the calculations lead to an abnormally deep imaginary potential with $W=40$ MeV and a diffuseness $a_I=0.3$ F. This potential does not seem reasonable and therefore has been discarded.

For the $W^{182}(d,p)W^{183}$ reaction at $E_d=12$ MeV, the energy of the ground-state proton group is 15.8 MeV; but the proton scattering from W^{183} was measured at a bombarding energy of 12 MeV. In comparing the results, therefore, the best-fit parameters obtained from our 12-MeV proton scattering were extrapolated to 15.8 MeV on the assumption that the energy depend-

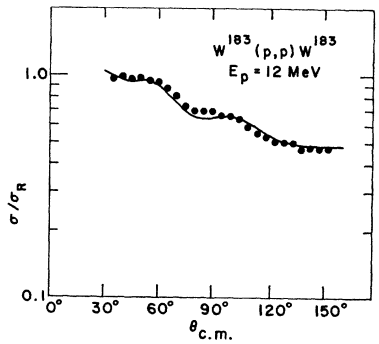

FIG. 3. Angular distribution of protons elastically scattered from W^{183} at $E_p=12$ MeV. Cross sections are given as σ/σ_R, the ratio to Rutherford scattering. The curve is an optical-model calculation with the "best fit" parameters obtained from the search on V and W. Except that $V=55.2$ MeV, all parameters are the same as those of potential $P1$ in Table II.

[17] F. G. Perey (unpublished).

[18] F. G. Perey, in Argonne National Laboratory Report ANL-6848, edited by F. E. Throw, p. 114 (unpublished).

[19] F. G. Perey, Phys. Rev. 131, 745 (1963).

TABLE IV. Optical-model parameters for the scattering of 15.8-MeV protons on W^{183} ($r_c=r_0=1.25$ F).

Potential	V (MeV)	r_0 (F)	a (F)	W (MeV)	r_{0I} (F)	a_I (F)	V_{LS} (MeV)
$P0$[a]	55.0	1.25	0.65	17.7	1.25	0.47	8
$P1$[b]	53.1	1.25	0.65	10.2	1.25	0.76	8

[a] Potential $P0$ is Perey's average proton potential (Ref. 19).
[b] Potential $P1$, is the one that best describes our scattering data (search restricted to V and W). The potential has been extrapolated to a proton energy of 15.8 MeV. ($V=55.2$ MeV at $E_p=12$ MeV.)

ence of the proton potential is as given by Perey[19] (i.e., $V=V'-0.55E_p$ and all other parameters are constant). The parameters of the extrapolated potential (potential $P1$) are listed in Table IV together with the "average" proton potential (potential $P0$) from Perey's survey[19] on proton scattering.

In contrast to the proton scattering from W^{183}, no satisfactory fit to our deuteron scattering data can be obtained with "average" geometrical parameters and with the search limited to the strengths of the real and the imaginary potentials (V and W). The "average" geometrical parameter set B of Perey and Perey[13] was chosen since it leads to a real potential whose strength V is roughly the sum of the potentials of the free neutron and proton. The failure to fit the deuteron-scattering data with these average geometrical parameters probably reflects the importance of strong-coupling effects caused by the large static deformation of W^{182}. If, on the other hand, the search is extended to include a and a_I, very good fits to our data can be obtained.

From a series of calculations of the deuteron scattering with different values of W and a search on V, a, and a_I, we find a serious ambiguity in V, W, a, and a_I: W can vary by a factor of 2 or more without seriously affecting the quality of the fits, but V, a, and a_I are only slightly affected by a considerable change in the choice of W. Figure 4 shows this dependence of V, a, and a_I on W. The "best-fit" angular distribution calculated with a shallow imaginary potential W shows faint oscillations which are damped out with increasing W. The differences in the predicted angular distributions, however, are not large enough to allow one to determine a set of parameters unambiguously from our 12-MeV scattering data. It is interesting to note further (Table V) that the

TABLE V. Optical-model parameters for the scattering of 12-MeV deuterons on W^{182} ($r_c=r_0=1.15$ F).

Potential	V (MeV)	r_0 (F)	a (F)	W (MeV)	r_{0I} (F)	a_I (F)	σ_R (mb)
$D0$[a]	104.0	1.15	0.810	13.5	1.34	0.680	766
$D1$[b]	116.7	1.15	0.810	12.7	1.36[d]	0.851	1010
$D2$[c]	113.7	1.15	0.901	22.6	1.36[d]	0.709	956

[a] $D0$ is the average deuteron potential B from Perey and Perey (Ref. 13).
[b] $D1$ is the "best fit" potential obtained from a search on V, W, and a_I.
[c] $D2$ is an alternative "best fit" potential from the search on V, W, a, and a_I. It is the one that gives minimum χ^2.
[d] The radius of the imaginary well has been adjusted to 1.36 F, which seems to be a slightly better value than 1.34 F for the rare-earth nuclei.

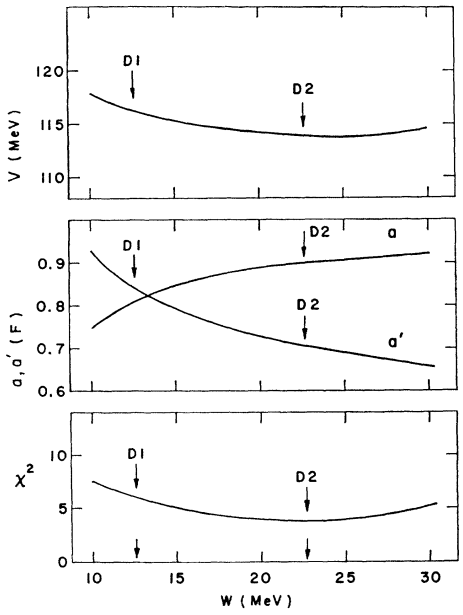

FIG. 4. Ambiguities in the deuteron optical potentials. The figure shows the best-fit parameters V, a, and a' together with χ^2 for a given imaginary well depth W. In these calculations $r_0=1.15$ F and $r_I=1.36$ F. $D1$ and $D2$ denote potentials used in the DWBA calculations.

reaction cross sections σ_R differ only insignificantly ($\sim 5\%$) for different values of W.

We have therefore somewhat arbitrarily chosen a deuteron potential by imposing the requirement that the real well should have the same geometrical parameters (r_0,a) as average potential B of Perey and Perey.[17] This choice leads to potential $D1$ whose parameters are given in Table V. Also listed in Table V is the potential $D2$ that gives the minimum χ^2 in a comparison of the calculated angular distributions with the data. In Fig. 5 the angular distribution calculated with potential $D1$ is compared with the deuteron scattering data. Also included (the dashed curve) is the angular distribution predicted by the average potential $D0$ of Perey and Perey,[17] since this potential has also been used in the DWBA analysis of our data. As can be seen from Fig. 5, the elastic deuteron scattering is not fitted with the average potential $D0$.

In Fig. 6 the differential cross sections for inelastic deuteron scattering to the first 2^+ level are compared with the angular distributions predicted by the DWBA theory. The theoretical angular distributions have been calculated with the Oak Ridge DWBA code JULIE.[20,21] Potential $D1$ has been used as the distorting potential in and DWBA calculations.[21a] It was assumed that both

[20] R. H. Bassel, R. M. Drisko, and G. R. Satchler, Oak Ridge National Laboratory Report ORNL-3240 (unpublished).
[21] R. H. Bassel, G. R. Satchler, R. M. Drisko, and E. Rost, Phys. Rev. 128, 2693 (1962).
[21a] *Note added in proof.* The inelastic scattering calculations were accidentally done with parameters slightly different from those shown in Table V for Potential $D1$ ($r_{0I}=1.34$F, $a_I=0.898$F).

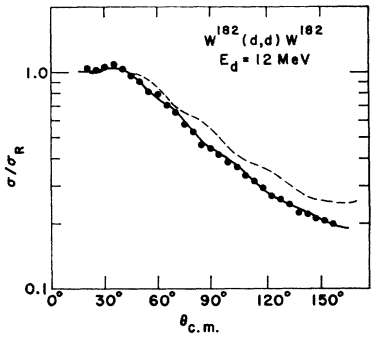

FIG. 5. Angular distribution of deuterons elastically scattered from W^{182} at $E_d=12$ MeV. The cross sections are given as σ/σ_R. The solid curve has been obtained from an optical-model calculation with the "best fit" parameters $D1$ of Table III. For comparison, the angular distribution calculated with Perey and Perey's "average" potential $D0$ from Table III has been included (dotted curve).

the real and the imaginary term of the optical potential are deformed (i.e., a complex interaction was used[22]). Coulomb excitation has been taken into account in the calculation. As has recently been shown,[22] a complex interaction is required to describe the inelastic scattering of strongly absorbed particles. This is also demonstrated by the present calculation. Figure 6 shows theoretical angular distributions which have been calculated with a real interaction only, with a real interaction with Coulomb excitation, and finally with a complex interaction with Coulomb excitation. The complex interaction with Coulomb excitation is required to reproduce both the magnitude and the shape of the measured angular

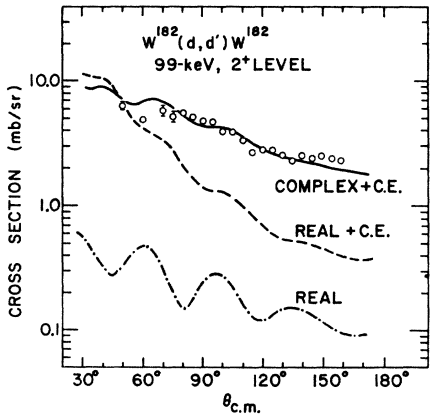

FIG. 6. Differential cross sections for inelastic deuteron scattering that leaves the W^{182} in its first 2^+ level. The curves are DWBA calculations with a deformed optical potential. Calculations have been performed with only the real potential deformed (REAL), a deformed real potential plus Coulomb excitation (REAL+C.E.) and finally with both the real and the imaginary well deformed and Coulomb excitation included (COMPLEX +C.E.). All calculations were done with the measured potential $D1$ and with $\beta=0.23$.

distribution. The calculation leads to a deformation parameter $\beta=0.23$ which may be compared with $\beta=0.24$ from Coulomb-excitation studies.[23] A DWBA calculation with potential $D2$ leads to $\beta=0.21$.

B. Intercomparison of the Measured (d,p) Angular Distributions

An examination of the (d,p) angular distributions in Fig. 7 shows that there are significant differences be-

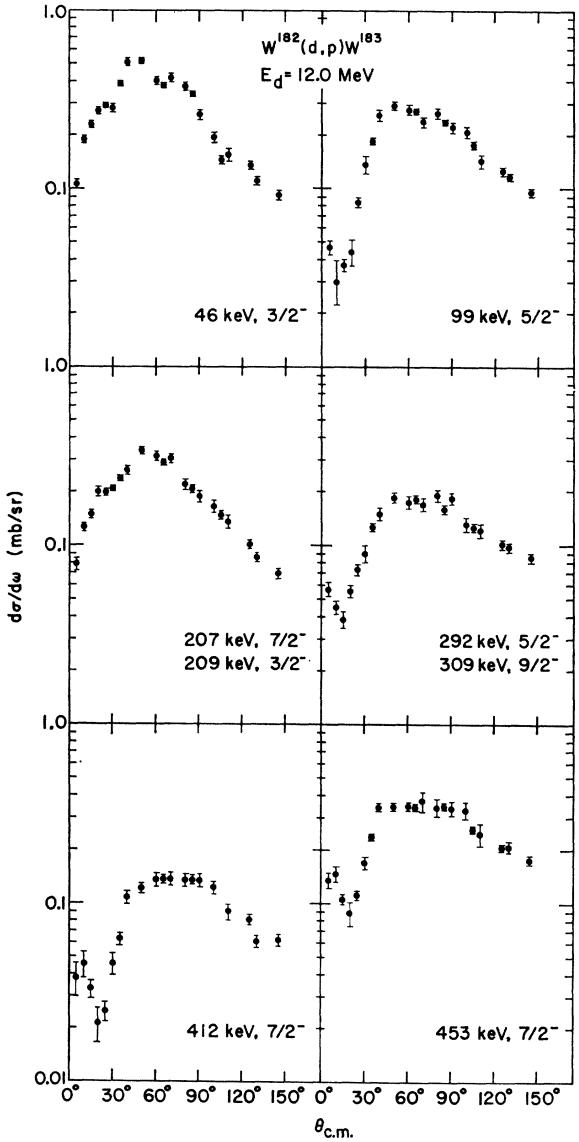

FIG. 7. Angular distributions of the protons from the W^{182}-$(d,p)W^{183}$ reaction leading to the levels at 46-, 99-, 208-, 292-, 412-, and 453-keV excitation in W^{183}. The deuteron energy was 12 MeV. The angular distribution of the weak ground-state transition is given in Fig. 15.

[22] H. W. Broek, J. L. Yntema, B. Buck, and G. R. Satchler, Nucl. Phys. **64**, 259 (1965); E. R. Flynn and R. H. Bassel, Phys. Rev. Letters **15**, 168 (1965).

[23] B. Elbek, *Determination of Nuclear Transition Probabilities by Coulomb Excitation* (Ejnar Munksgaards Forlang, Copenhagen, 1963).

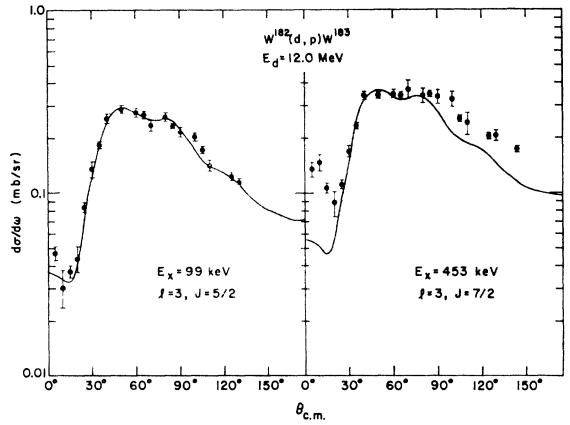

FIG. 8. Comparison of the angular distributions of the $l=3$ transitions to the levels at 99- and 453-keV excitation in W^{183}. The two transitions differ in their total angular-momentum transfer, which is $j=\frac{5}{2}$ for the transition to the 99-keV level and $j=\frac{7}{2}$ for the transition to the 453-keV level. The solid curves were obtained from spin-dependent DWBA calculations with potentials *D2P1*. Spin-orbit coupling has been included for the proton and for the captured particle.

tween some angular distributions of transitions with the same orbital angular momentum l and in some cases even with the same total angular-momentum transfer j. These differences are most pronounced for the $l=3$ transitions to the 99- and 454-keV levels in W^{183}, which are compared in Fig. 8. The angular distribution of the transition to the 99-keV $I=\frac{5}{2}$ level has a deeper minimum at far forward angles and also decreases faster in magnitude towards backward angles than the angular distributions of the transition to the $I=\frac{7}{2}$ level at $E_x=453$ keV. Figure 8 also includes theoretical angular distributions calculated with a spin-dependent DWBA code. The Q value appropriate to each transition has been used. These calculations are discussed in more detail in Sec. IIIB. From the comparison of the data with the DWBA calculations, we find that the observed differences in the angular distributions cannot be explained by differences in the Q values. Since the transitions to the 99- and 453-keV levels differ by the total angular momentum j of the transferred neutron in the (d,p) reaction, it initially had been suspected that the differences in the angular distributions reflect j-dependent effects similar to those found by Lee and Schiffer[24] in (d,p) reactions on medium-weight nuclei. Since, however, there are also differences between the angular distributions of the transitions to the 412- and 453-keV levels which have same l and j, as can be seen in Fig. 9, the explanation of the differences solely in terms of j dependence appears less certain. Still, the angular distribution of the $j=\frac{7}{2}$ transition to the 412-keV level bears a closer resemblance to the angular distribution of the transition to the 453-keV level than to that of the $j=\frac{5}{2}$ transition to the 99-keV state.

[24] L. L. Lee, Jr., and J. P. Schiffer, Phys. Rev. Letters **12**, 108 (1964); Phys. Rev. **136**, B405 (1964).

The second known $j=\frac{5}{2}$ transition in the $W^{182}(d,p)W^{183}$ reaction to the level at 292-keV excitation is unfortunately only partially resolved from the transition to the $I=\frac{9}{2}$ level at 309-keV excitation. If, however, the contribution from the $l=5$ transition is subtracted from the sum angular distribution at forward angles (where the two groups are best separated), the angular distribution (not shown) of the $j=\frac{5}{2}$ transition to the 292-keV level has the same deep minimum at forward angles as the $j=\frac{5}{2}$ transition to the 99-keV state. Both $j=\frac{5}{2}$ angular distributions are then indeed very similar.

Differences in the angular distributions are also found for the $l=1$ transitions to the levels at 46- and 209-keV excitation (see Fig. 9), although here the situation is not quite as certain since a small portion of the 209-keV angular distribution is presumably due to the weak $l=3$ transition to the $I=\frac{7}{2}$ state at 207 keV. The differences in the angular distributions persist, however, if the $l=3$ angular distribution of the transition to the 207-keV state is subtracted. For this subtraction the spectroscopic factor of the 207-keV level was taken to be that calculated from the rotational model as discussed in Sec. IIIE.

As is seen from Fig. 9, the $l=1$ transition to the 46-keV level has a sharp maximum at 40° which is not observed in the angular distribution of the transition to the 209-keV level. Also, there are more oscillations in the angular distribution of the transition to the 46-keV level than in the transition to the 209-keV level. Since the same total angular-momentum transfer is involved in both transitions, the differences between the angular distributions cannot be explained by j dependence. Aside from the differences in Q value (which, however, are negligible), the two transitions differ only in that the

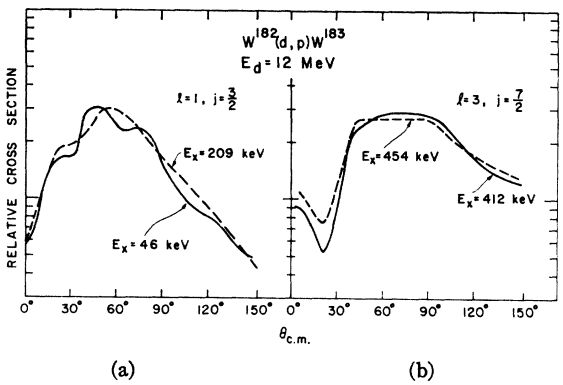

FIG. 9. Angular distributions of the (d,p) reaction at $E_d=12$ MeV: (a) the $l=1$ transitions to the levels at 46- and 209-keV excitation, (b) the $l=3$ transitions to the levels at 412- and 454-keV excitation. The total angular-momentum transfer is $j=\frac{3}{2}$ for both $l=1$ transitions and $j=\frac{7}{2}$ for both $l=3$ transitions. The solid curves have been obtained by drawing a curve through the experimental points. By assuming the strength of the $l=3$ transition to be that calculated from the Nilsson wave functions with the inclusion of band-mixing and pairing the contribution from the weak and unresolved $l=3$ transition to the 207-keV level has been subtracted from the predominantly $l=1$ sum of the angular distributions of the transitions to the 207- and 209-keV levels.

rotational bands into which the neutron is captured are different. An explanation which therefore comes to mind is that the observed differences in the angular distributions might be due to configuration-mixing effects,[25,26] which may change the shape of the bound-state wave function. If the observed differences between two angular distributions of the same l and j are due to such configuration-mixing effects, then similar differences in the angular distributions should be observed in transitions to the same rotational bands in neighboring nuclei. Alternatively, the differences in the angular distributions with the same l and j may be caused by inelastic-scattering effects. Such effects will be discussed in Sec. IIID.

C. DWBA Analysis of the Data

1. Computational Methods

DWBA calculations of the (d,p) angular distributions have been made with a spin-dependent stripping code and with a spin-independent version of this program which have been written by Macefield.[27] Because of the longer computing time required for the spin-dependent calculations, most calculations were done with the spin-independent code. Both DWBA codes use the zero-range modified Born approximation. The bound-state wave function of the captured particle is computed from a Woods-Saxon well whose depth is adjusted to give the correct separation energy. The radius and diffuseness of the well for the calculation of the bound-state wave function have been chosen to be 1.25 and 0.65F, respectively. A Hulthén-type wave function was assumed for the deuteron. Since the effect of a cutoff radius on the calculated angular distributions was found to be small with the optical-model potentials chosen, it can be expected[28] that effects of nonlocality and finite range will alter our results only insignificantly. Consequently, nonlocality and finite-range effects have not been considered. All calculations presented have been done without a cutoff radius. The optical-model parameters used in the calculations were either those for potentials $D1$, $D2$, and $P1$ obtained from the scattering measurements at 12 MeV as discussed above or for Perey's average potentials $D0$ and $P0$. All potentials are listed in Tables IV and V.

2. Comparison Between the DWBA Calculations and the Data

For a comparison of the DWBA calculations with the data, we have chosen the transitions to the first and second excited states in W^{183}, which are reached by $l=1$ and $l=3$ stripping, respectively. In view of the differences mentioned above between angular distributions with the same l, the restriction to these two transitions introduces an element of arbitrariness. A set of potentials that gives an excellent fit to one transition may give poorer fits to the others. Since the differences between the angular distributions from transitions having the same l but going to different final states are apparently not accounted for by the ordinary DWBA, the differences reflect the accuracy within which we can expect the DWBA to reproduce the data.

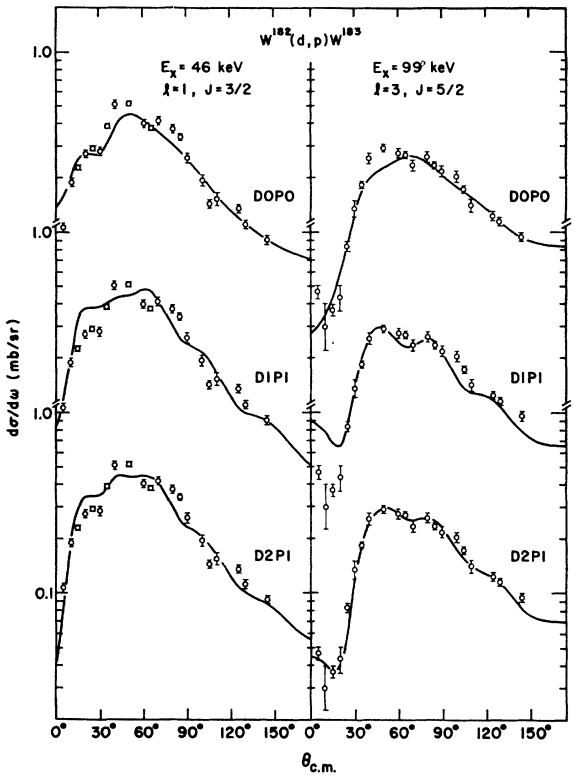

FIG. 10. Comparison between the data and the DWBA calculations with different distorting potentials for the $l=1$ transition to the first excited state in W^{183} and the $l=3$ transition to the second. Potentials $D1$, $D2$, and $P1$ were obtained from the optical-model analysis of our elastic-scattering measurements. Potentials $D0$ and $P0$ are average potentials as found by Perey and Perey (Ref. 13) and by Perey (Ref. 19).

In Fig. 10, DWBA calculations with potentials $D0P0$, $D1P1$, and $D2P1$ are compared with the data. Although the angular distributions calculated with the different potentials differ significantly from each other, they all agree about equally well with the data. In particular, the measured potential $D2P1$ gives an excellent fit for the $l=3$ transition to the state at 99 keV, whereas the $l=1$ angular distribution calculated with the average Perey potential $D0P0$ seems to reproduce the observed $l=1$ distributions better. In view of the differences between the measured angular distributions, the over-all agreement observed with the DWBA calculations is probably as good as one can expect. Thus a comparison between the measured and the calculated angular

[25] N. Austern, Phys. Rev. 136, B1743 (1964).
[26] W. T. Pinkston and G. R. Satchler, Nucl. Phys. 72, 537 (1965).
[27] B. E. Macefield (unpublished).
[28] N. Austern, R. M. Drisko, E. C. Halbert, and G. R. Satchler, Phys. Rev. 133, B3 (1964).

distributions at 12 MeV appears to be insufficient to determine which potentials should be used for the DWBA analysis. This question is of interest in view of strong-coupling effects, which should be present in the $W^{182}(d,p)W^{183}$ reaction. The potentials $D0P0$ represent average spherical potentials which describe the elastic scattering in the absence of strong-coupling effects, whereas these effects are included in the potentials $D1$, $D2$, and $P1$ obtained from a fit to the elastic-scattering data from W^{182} and W^{183}, respectively.

At 7.5-MeV bombarding energy, the angular distributions calculated with parameter sets $D0P0$, $D1P1$, and $D2P1$ differ insignificantly from each other in shape. These 12-MeV potentials were used since it was not known how to extrapolate the potentials to 7.5 MeV. In Fig. 11 the experimental angular distributions of the $l=1$ and $l=3$ transitions to the 45- and 991-keV states are compared with the DWBA curves calculated from the parameter set $D2P1$. The theoretical curves do not fit the "front edge" of the angular distributions correctly—the experimental cross sections decrease faster towards forward angles than theoretically predicted.

The theoretical curves in Figs. 10 and 11 have been calculated without spin-orbit coupling. As is seen from Fig. 8, the inclusion of spin-orbit coupling in the distorting potentials as well as in the calculation of the bound-state wave function has very little effect on the shapes of the theoretical curves. The distributions in Fig. 8 were calculated with the measured potentials $D2P1$. The main effect of the spin-orbit coupling is to increase (decrease) all cross sections for $j=l+\frac{1}{2}$ ($j=l-\frac{1}{2}$) of the captured particle. For $l=1$ capture, the increase is less than 5% for $j=l+\frac{1}{2}$ and the decrease is approximately 12% for $j=l-\frac{1}{2}$. For $l=3$ capture, the corresponding numbers are +10% for $j=l+\frac{1}{2}$ and 20% for $j=l-\frac{1}{2}$.

D. Inelastic-Scattering Effects

Because of the large permanent deformation of the tungsten isotopes, one might expect inelastic-scattering (strong-coupling) effects to play a role in the $W^{182}(d,p)W^{183}$ reaction. Since we do not know the true distorting potentials (as discussed above) it appears difficult if not impossible to assess the importance of these second order effects solely from a comparison of the measured angular distributions with the DWBA calculations. As was mentioned above, however, the differences between angular distributions of the same l and j might be due to such inelastic-scattering effects.

Inelastic-scattering effects result from the strong coupling of inelastic-scattering channels to the initial and/or final state in the stripping process. They will affect the elastic scattering and with it the distorted waves. To first order, however, these effects are taken into account by extracting optical potentials from the measured elastic scattering. In addition, the inelastic scattering will contribute two-step processes to the reaction amplitude. From the good agreement between the shapes of the measured and the calculated (d,p) angular distributions, it must be concluded that the effects of the two-step processes are either unimportant or that the angular distributions from the combined ordinary and two-step stripping process are not very different from the angular distributions of ordinary stripping.

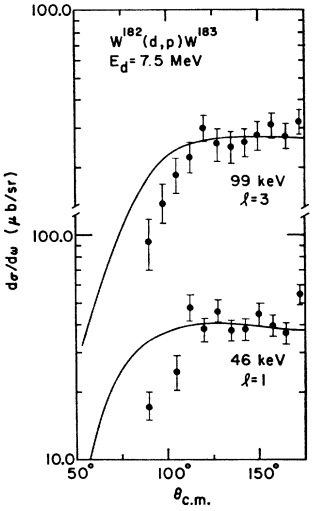

FIG. 11. Angular distributions of the proton groups leading to the first and second excited state in W^{183} formed by the $W^{182}(d,p)W^{183}$ reaction at $E_d=7.5$ MeV. The solid curves were obtained from a DWBA calculation with the measured potentials $D2P1$.

Inelastic scattering effects have been investigated theoretically[5,6] by several authors. Penny and Satchler[5] considered the strong coupling of the first 2^+ states only, which might be either rotational or vibrational states. In Iano's calculations,[6] on the other hand, the strong coupling is taken into account in the adiabatic approximation between all states of the rotational bands, of which the initial and final states are members. Some experimental evidence for two-step processes was recently found by Bock *et al.*,[29] and Belote *et al.*[30]

Preliminary calculations by Penny and Satchler[31] of strong-coupling effects in the $W^{182}(d,p)W^{183}$ reaction indicate that for the strong transitions the contributions from two-step processes are indeed negligibly small. For the transition to the first and second excited states in W^{183}, the latter authors find that angular distributions calculated with and without inelastic-scattering effects differ from each other by less than 10% except at the far backward angles. The differences are well within the other uncertainties of the DWBA calculation. In their calculations, Penny and Satchler,[31] considered only the strong coupling to the 2^+ state of the target nucleus. Also only one l' value ($l=1$) was taken into account in the calculation of the two-step process. The reaction amplitude can then be written as the sum of the amplitudes for direct stripping (subscript D) and for a

[29] R. Bock, H. H. Duhm, R. Rudel, and R. Stork, Phys. Letters **13**, 151 (1964).
[30] T. A. Belote, W. E. Dorenbusch, O. Hansen, and J. Rapaport, Nucl. Phys. **73**, 321 (1965).
[31] S. K. Penny and G. R. Satchler (private communication).

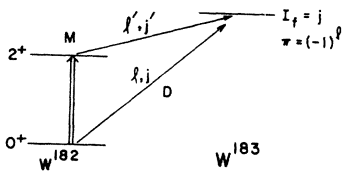

FIG. 12. Diagram illustrating the angular momenta transferred in the direct and in the "two-step" (multiple) stripping process via the first 2^+ level in the target nucleus.

"multiple" transition (subscript M) with angular momenta (l,j) and (l',j) (Fig. 12). The differential cross section is given by the expression[5]

$$d\sigma/d\Omega=(2J_f+1)(X_D^2\sigma_D+X_M^2\sigma_M+2X_DX_M\sigma_{DM}),$$

and

$$X_D=\theta_{jl},\quad X_D^2=S_{lj},$$

$$X_M=\sum\theta_{j'l}(-1)^{j'+l-\frac{1}{2}}[(2l+1)(2j'+1)]^{1/2}W(jj'll',2\tfrac{1}{2}),$$

where θ_{jl} is the reduced width, S_{jl} is the spectroscopic factor, and σ_D and σ_M are the direct and "multiple" stripping cross sections. The potentials used in the calculation by Penny and Satchler[31] are given in Table VI. The parameter set d(SPH) is the deuteron potential used for the calculation of the direct transition; d(DEF) is the potential which in a strong-coupling calculation with $\beta=0.3$ gives the same angular distribution for the elastic scattering as potential d(SPH) gives with the spherical optical model. The strong-coupling code used by Penny and Satchler[31] included no provision for a complex interaction, which is known to increase the cross section for inelastic scattering and the calculations also neglect Coulomb excitation. To compensate for this, they chose $\beta=0.3$ for the strong-coupling calculation instead of using the value $\beta=0.24$ obtained from Coulomb excitation. Figure 13 shows the differential cross sections for ordinary stripping and for the two-step process as calculated by Penny and Satchler.[31] The cross sections for the two-step processes are two orders of magnitude smaller than the cross sections of the strong transitions in ordinary stripping. Therefore, two-step processes should only be important for transitions for which the direct stripping is highly forbidden.

TABLE VI. Deuteron and proton potentials used in the strong-coupling calculations by Penny and Satchler (Ref. 29).

	V (MeV)	r_0 (F)	a (F)	W_D (MeV)	r_I (F)	a_I (F)
d(SPH)	104.0	1.15	0.81	13.5	1.34	0.68
d(DEF)	113.4	1.15	0.81	17.8	1.285	0.68
p	53.0	1.25	0.65	18.0	1.25	0.47

Such a situation exists for the transition to the ground state in the $W^{182}(d,p)W^{183}$ reaction. Because of angular-momentum conservation, the ground state can only be formed by capture of the stripped neutron with $l=1$ and $j=\frac{1}{2}$ in the (d,p) reaction. According to the Nilsson model of the wave functions, the intensity of the $l=1$, $j=\frac{1}{2}$ component of the $[510]\frac{1}{2}$ intrinsic state, however, should be only about a fiftieth of the intensity of the $l=1$, $j=\frac{3}{2}$ component. In Fig. 14 the measured angular distribution of the transition to the ground state is

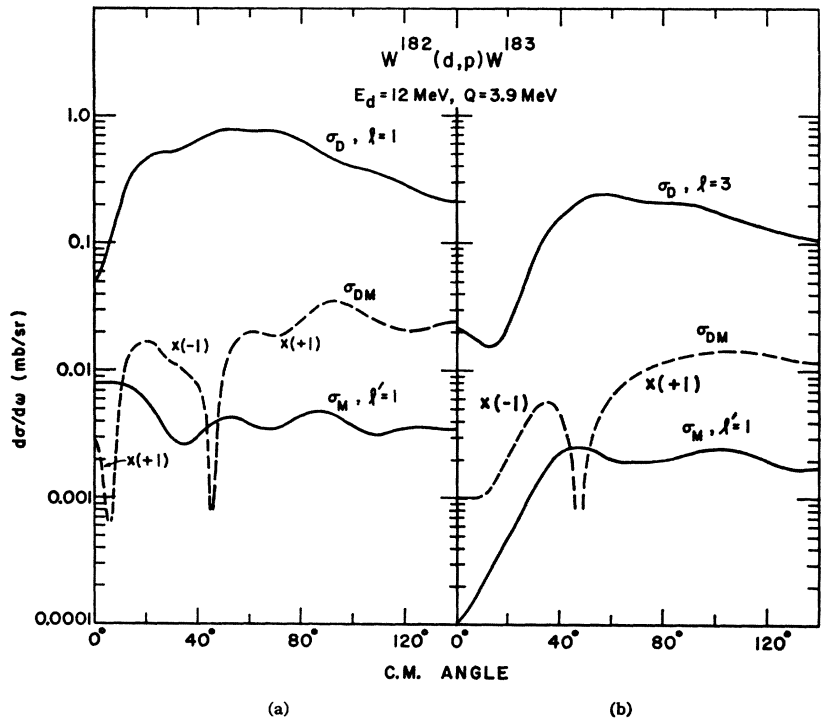

FIG. 13. Differential cross sections calculated by Penny and Satchler (Ref. 31) for the $W^{183}(d,p)W^{183}$ reaction for the "direct" (σ_D) and the "multiple" (σ_M) transition as well as for the interference term between the "direct" and the "multiple" transitions (σ_{DM}). In Fig. 13(a), $l=l'=1$. In Fig. 13(b), $l=3$ and $l'=1$.

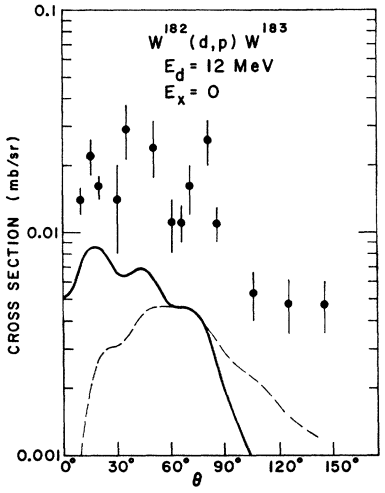

FIG. 14. Comparison of the experimental points and the calculated angular distribution curves for the ground-state transition in the $W^{182}(d,p)W^{183}$ reaction. The solid curve [calculated by Penny and Satchler, Ref. 3] includes the effects of inelastic scattering. The dashed curve is the angular distribution predicted by the ordinary DWBA theory without strong-coupling effects. For the ground-state transition $X_D=0.054$ and $X_M=0.57$.

compared with the angular distribution derived from the calculations by Penny and Satchler.[31] Unfortunately, the data on the ground-state transition are rather poor because of the small cross section involved. At forward angles the agreement in shape between theory and experiment is somewhat improved when two-step processes are included.

The predicted angular distributions depend sensitively on the sign of the interference term. Since the strong-coupling calculations by Penny and Satchler use a real interaction, whereas it is known from inelastic-scattering measurements that a complex interaction should be taken, uncertainties arise in the sign and the magnitude of the interference term and enter into the shape of the predicted angular distribution.

The predicted cross sections, however, are still found to be too low by a factor of 2–3 if two-step processes are included. This lack of agreement in the magnitude of the cross section may not be significant, since there is at least a factor-of-two uncertainty in the predicted cross section because of an uncertainty in the ground-state wave function of W^{183}. (This point is discussed further in the Appendix.) In addition, the calculations by Satchler and Penny[31] have been done with a truncated model (strong coupling only in the entrance channel to one excited state and restriction to one l' value in the multiple-stripping process).

From the ratio of the measured cross sections for transitions to the ground state and the first excited state, an upper limit on the importance of two-step processes in the $W^{182}(d,p)W^{183}$ reaction can be obtained by assuming that the ground state is reached only by two-step processes. The upper limit thus obtained is less than 10% of the intensity of the transition to the first excited state near the maximum of the $l=1$ angular distribution. To obtain this number, the spin factor has already been divided out. The upper limit derived from our data is probably still too large, since 10% in the cross section corresponds to 30% in the reaction amplitude. Because of the interference between the direct and the two-step amplitudes, the 30% admixture in the reaction amplitude would lead one to expect more than the observed differences in shape among angular distributions with the same values of l and j.

Our results show the difficulties in assessing the importance of second-order effects. In order to obtain a quantitative estimate of the two-step processes, one has to deal with transitions that are highly forbidden for the "direct" stripping mode. Then, however, small admixtures to the wave function of the final state become important; and these cannot be accurately predicted with present theories.

E. Spectroscopic Factors

Spectroscopic factors have been extracted from the data by a comparison with the predicted cross sections from the DWBA calculations. To investigate the influence of the distorting potentials on the spectroscopic factors, calculations have been done with several distorting potentials and with different combinations of these deuteron and proton potentials, namely potentials *D0P0*, *D1P1*, *D2P1*, *D0P1*, *D1P0*, and *D2P0*. Table VII lists the theoretical spectroscopic factors for transitions to the first and second excited states and compares these with the values extracted from the data by use of the spin-independent code. A discussion of the calculation of the theoretical spectroscopic factors will be found in the Appendix.

Good agreement is found between the experimental and theoretical ratios of the spectroscopic factors of the first and second excited states, the experimental ratios being quite insensitive to the choice of the distorting potentials. The absolute values of the experimental spectroscopic factors, on the other hand, depend strongly on the distorting potentials.[32] All experimental spectroscopic factors (from the 7.5-MeV data as well as from the 12-MeV data) were found to be larger than the theoretically predicted spectroscopic factors. The spectroscopic factors extracted with DWBA calculations that use the average Perey potentials *D0P0* agree best with the theory, whereas the spectroscopic factors obtained from the calculations with the measured potentials are sometimes as much as twice the theoretical spectroscopic factors. It is further interesting to note that the combinations *D0P1*, *D1P0*, and *D2P0* of the "average" with the measured potentials give spectroscopic factors which are also too large.

Whether the success of the calculation with the

[32] Variation in the absolute spectroscopic factors by as much as a factor of 2 were also found in the analysis of the $Pb^{206}(d,p)Pb^{207}$ reaction by W. R. Smith, Phys. Rev. 137, B913 (1965).

TABLE VII. Comparison of spectroscopic factors for transitions to the first and second excited states of W^{183}. The values shown were extracted from the data taken at $E_d=7.5$ and 12.0 MeV with the aid of different distorting potentials.

Transition	S_{theor}	$E_d=7.5$ MeV			$E_d=12.0$ MeV					
		D0P0	*D1P1*	*D2P1*	*D0P0*	*D1P1*	*D2P1*	*D0P1*	*D1P0*	*D2P0*
$l=1$, $Q=3.92$ MeV	0.117	0.13	0.19	0.17	0.15	0.25	0.25	0.20	0.22	0.22
$l=3$, $Q=3.86$ MeV	0.168	0.16	0.23	0.22	0.20	0.33	0.35	0.28	0.29	0.29
S_3/S_1	1.43	1.25	1.20	1.30	1.35	1.30	1.40	1.40	1.30	1.30

"average" potentials *D0P0* is just fortuitous or whether it bears some physical significance cannot be decided until more measurements are made on other nuclei. The "average" potentials can be looked at as the potentials that would describe the scattering from tungsten in the absence of strong-coupling effects, whereas the measured potentials include the effects of strong coupling. Heretofore the understanding has been that the measured potentials should be taken for the DWBA calculations in order to obtain the correct spectroscopic factors. However, the present results cast some doubt on this expectation.

The above result, namely that the spectroscopic factors extracted from the data with a DWBA analysis are larger than the theoretical spectroscopic factors, is also implicit in the data of Macefield and Middleton[4] who studied the $U^{238}(d,p)U^{239}$ reaction at 12 MeV. The optical parameters which they use, however, were not measured for these particular nuclei, but were taken from scattering measurements on gold. The potentials were arbitrarily adjusted to give a good fit to the shape of the measured (d,p) angular distributions. If the theoretical spectroscopic factors for the $U^{238}(d,p)U^{239}$ reaction are calculated according to the methods outlined in the Appendix, and if reasonable estimates for the pairing are included, then the spectroscopic factors extracted with the DWBA analysis are roughly twice the theoretical spectroscopic factors. This discrepancy is in the same direction and is of about the same size as found in the present study of $W^{182}(d,p)W^{183}$ reaction when our measured optical potentials are used.

In Table VIII, the theoretical spectroscopic factors for all levels in W^{183} up to 453-keV excitation are compared with the experimental spectroscopic factors from the data at 12 MeV. The experimental spectroscopic factors were extracted by use of DWBA calculations with the measured potentials *D2P1*. The results from both spin-independent and spin-dependent calculations have been listed. Under the heading S_{calc} in Table VIII, column (a) lists the theoretical spectroscopic factors calculated from the single-particle rotational model with Nilsson wave functions and without band mixing or pairing. The spectroscopic factors in column (b) include the effects of band mixing, and in column (c) the effects of the pairing interactions have also been taken into account. The details of the calculation of the spectroscopic factors are discussed in the Appendix. Figure 15 is a plot of the ratios of the experimental and the theoretical spectroscopic factors from Table VIII. These ratios will be equal to unity if both the theoretical spectroscopic factors and the DWBA cross sections are correctly predicted.

The ratios of the spectroscopic factors calculated without band mixing and pairing corrections fluctuate widely [Fig. 15(a)]. If band mixing is taken into account, however, the ratios of the spectroscopic factors are seen to differ much less from one state to the other [Fig. 15(b)]. This result underlines the importance of treating band mixing in the calculation of the wave functions of W^{183}. The scatter of the ratios of the spectroscopic factors is not further reduced if the effects of the pairing interaction are also included. The main effect of the pairing is to increase the ratios of the spectroscopic factors.

TABLE VIII. Calculated and measured spectroscopic factors for W^{183}. The experimental values were extracted from the 12-MeV data; the theoretical values were obtained by DWBA calculations with potentials *D2P1*.

E_x (keV)	K	I	S_{calc}[a] (a)	(b)	(c)	(d)	S_{exp}[b] (e)	(f)	(g)	(h)
0.0	$\frac{1}{2}$	$\frac{1}{2}$	0.004	0.004	0.003	0.03				
46	$\frac{1}{2}$	$\frac{3}{2}$	0.22	0.164	0.117	1.0	0.25	1.0	0.25	1.0
99	$\frac{1}{2}$	$\frac{5}{2}$	0.105	0.224	0.168	1.44	0.35	1.38	0.42	1.7
208	$\frac{1}{2}$	$\frac{7}{2}$	0.037	0.009	0.006	0.05				
209	$\frac{3}{2}$	$\frac{3}{2}$	0.055	0.116	0.093	0.80	0.16	0.63	0.16	0.64
292	$\frac{3}{2}$	$\frac{5}{2}$	0.223	0.113	0.100	0.85	0.21	0.83	0.25	1.0
309	$\frac{1}{2}$	$\frac{9}{2}$	0.015	0.033	0.026	0.22				
412	$\frac{3}{2}$	$\frac{7}{2}$	0.023	0.051	0.040	0.34	0.11	0.43	0.10	0.40
453	$\frac{7}{2}$	$\frac{7}{2}$	0.230	0.230	0.209	1.78	0.31	1.22	0.28	1.1

[a] The four calculated spectroscopic factors given for each level were obtained (a) with no corrections for the effects of pairing and band mixing, (b) with corrections for band mixing included, and (c) with corrections for both band mixing and pairing included. The values in column (d) are the relative spectroscopic factors deduced from column (c).

[b] The experimental spectroscopic factors given in columns (e) and (f) are the absolute and relative values, respectively, extracted with the spin-independent DWBA code. Those in columns (g) and (h) are the absolute and relative values, respectively, extracted with the spin-dependent DWBA code.

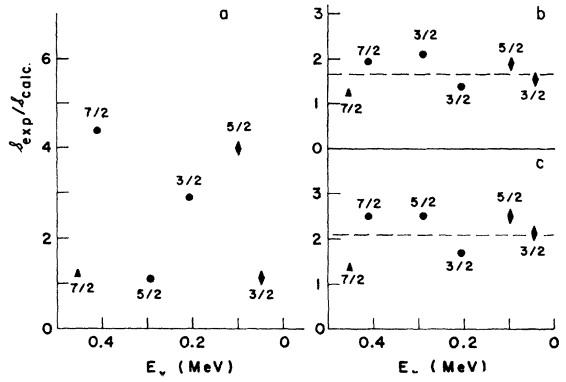

FIG. 15. Ratios of spectroscopic factors (S_{exp}/S_{theor}) obtained for the states studied in W^{183}. The theoretical spectroscopic factors in Fig. 15(a) were obtained from the rotational model without taking pairing and band mixing into account. Band mixing has been included in Fig. 15(b); and in 15(c), pairing interaction has also been taken into account. The experimental spectroscopic factors of Fig. 15(a), (b), and (c) were extracted with spin-dependent DWBA calculations.

The experimental spectroscopic factors of Fig. 15 are those extracted with the spin-dependent DWBA calculations; but the scatter of the ratios of spectroscopic factors appears to be somewhat less if the spectroscopic factors from the spin-independent calculations are used instead. Whether this indicates configuration-mixing effects[25,26] cannot be decided from the present data. The influence of such configuration-mixing effects on the bound-state wave function in the DWBA calculation is of considerable interest. As already mentioned, the binding energy of the captured particle was taken in all our calculations to be equal to the separation energy of the odd particle in contrast to employing the effective binding energy.[33] The latter method does not seem appropriate to our investigation, since at bombarding energies near the Coulomb barrier the main contribution to the reaction amplitude is given by the asymptotic tail of the bound-state wave function.

The remaining discrepancies in the relative spectroscopic factors are most likely due to the following causes.[26] In the Nilsson model,[34] which was used to calculate the theoretical spectroscopic factors, the intrinsic wave functions are expanded in terms of the three-dimensional harmonic oscillator, whereas the bound-state wave function in the DWBA theory is calculated from a real Woods-Saxon well. It is further assumed that all levels of a rotational band have the same intrinsic wave functions (adiabatic approximation[34]), which is only true if the levels are degenerate in energy. In order to be consistent, the same wave functions should be used both for the calculation of the theoretical spectroscopic factors and for the bound-state wave function in the DWBA. Such calculations will be feasible[35] in the near future.

IV. SUMMARY AND CONCLUSIONS

Relative spectroscopic factors extracted by means of the DWBA theory agree fairly well (within 30% for most strong transitions) with those predicted by the rotational model. A similar result has been obtained by Burke *et al.*[36] The relative spectroscopic factors do not depend sensitively on the choice of the distorting potentials in the DWBA calculation. Absolute spectroscopic factors, on the other hand, may be in error by as much as a factor of two or three. The measured spectroscopic factors were found to be consistently larger than those given by the theory.[37]

Measured angular distributions of the same l value show small but real differences one from another. This may be a j-dependent effect, although differences were also observed between angular distributions of the same l and j. This latter effect may be due to configuration mixing or to two-step processes.

Our results indicate that two-step processes in the reaction studied are probably unimportant.

ACKNOWLEDGMENTS

We are indebted to S. K. Penny and G. R. Satchler for making their strong-coupling calculations available to us prior to publication and for allowing us to include parts of their calculations in this paper. We wish to thank F. G. Perey for his program JIB3 and B. Macefield for his DWBA codes which we used in the analysis of our data. We also thank R. C. Barrett for his assistance with the strong-coupling calculations of the inelastic scattering and R. H. Bassel for performing the JULIE calculation.

APPENDIX: CALCULATION OF THEORETICAL SPECTROSCOPIC FACTORS FOR THE $W^{182}(d,p)W^{183}$ REACTION

The differential cross section for a deuteron stripping reaction on an even-even target may be written as

$$d\sigma/d\Omega = (2I+1)S_{jl}\phi_l(\theta), \qquad \text{(A1)}$$

[33] R. Sherr, E. Rost, and M. E. Rickey, Phys. Letters **12**, 420 (1964).

[34] S. G. Nilsson, Kgl. Danske Videnskab. Selskab, Mat. Fys. Medd. **29**, No. 16 (1955).

[35] T. Tamura (private communication); E. Rost (private communication).

[36] D. G. Burke, B. Zeidman, B. Elbek, B. Herskind, and M. Oleson (to be published).

[37] Dr. Satchler has pointed out, that part of the discrepancy between the measured and the theoretical spectroscopic factors may be removed if the following corrections to the DWBA are taken into account: (1) Recent investigations indicate that the deuteron normalization factor is 1.65 to 1.7 instead of the commonly used 1.5, which has been employed in this paper. (2) If the potential for the bound state wave function is nonlocal, the wave function is damped in the interior region of the nucleus, but the exterior tail has to be increased to preserve normalization. In the $A=90$ mass region this increase in the tail was found to increase the predicted cross sections by as much as 40%. In W^{183} this effect might even be larger.

where I is the total angular momentum of the final state, l and j are the orbital and total angular momentum, respectively, of the captured neutron, S_{jl} is the spectroscopic factor containing information about nuclear structure, and $\phi_l(\theta)$ is the intrinsic single-particle differential cross section. The spectroscopic factor S_{jl} can be written in terms of the reduced width amplitude θ_{jl} as $S_{jl}=\theta_{jl}^2$. If one assumes the single-particle model of an odd nucleon strongly coupled to a symmetric deformed core (i.e., the single-particle rotational model), one can express the reduced width amplitude[38] as

$$\theta_{jl}=[2/(2I+1)]^{1/2}\langle\phi_2|\phi_1\rangle C_{jl}, \quad \text{(A2)}$$

where C_{jl} is the amplitude in an expansion of the deformed single-particle wave function χ in terms of spherical-limit eigenfunctions ψ_{jl} (i.e., $\chi=\sum C_{jl}\psi_{jl}$). The factor $\langle\phi_2|\phi_1\rangle$ is the overlap of initial and final vibrational states and is assumed to be equal to unity for transitions leading to low-lying states. Values for the C_{jl} are usually taken from the Nilsson wave functions[34] of deformed single-particle states.

If two single-particle states are present with quantum numbers K differing by one or if both states have $K=\frac{1}{2}$, then rotational particle coupling (RPC) will produce mixing between the rotational bands built on these intrinsic states. (The quantum number K is the projection of the total angular momentum I on the symmetry axis.) The wave function of the mixed state can be written $\chi=\sum a_i\chi_{K_i}$, where a_i is the amplitude of the ith state with quantum number K_i. If band mixing is present, the reduced-width amplitude becomes

$$\theta_{jl}=[2/(2I+1)]^{1/2}\sum_i a_i C_{ijl}. \quad \text{(A3)}$$

The calculation of the spectroscopic factors should also include the effects of the pairing interaction, which mixes together the various single-particle states. The pairing interaction has the gross effect of reducing the cross sections to particle states in (d,p) reactions since the single-particle states in the even-even target are partially filled by the pairing and hence are unavailable to the captured neutron. With this refinement, the reduced-width amplitude becomes

$$\theta_{jl}=[2/2I+1]^{1/2}\sum_i a_i U_i C_{ijl}, \quad \text{(A4)}$$

where U_i^2 is the probability that a particular single-particle state is filled.[39] The U_i^2 were evaluated with the BCS pairing theory, in the manner described below. When band mixing and the pairing interaction are taken into account, the expression for the spectroscopic factor becomes

$$S_{jl}=[2/(2I+1)][\sum_i a_i U_i C_{ijl}]^2. \quad \text{(A5)}$$

Values for the spectroscopic factors in the W^{182}-$(d,p)W^{183}$ reaction can be obtained by evaluating Eq. (5). The results for the low-lying levels of W^{183} which arise from the $[510]\frac{1}{2}^-$, $[512]\frac{3}{2}^-$, and $[503]\frac{7}{2}^-$ intrinsic states are presented in Table VIII. The parameters used in the calculation were chosen as follows.

A set of values of a_i that account for the band mixing between the $[510]\frac{1}{2}^-$ and $[512]\frac{3}{2}^-$ states have been determined by Kerman[40] and by Brockmeier *et al.*[41] who fitted the precisely measured energies of the low-lying levels in W^{183} with the single-particle rotational model. The mixing parameters of Brockmeier *et al.*,[41] lead to values of a_i that differ from Kerman's values (used in the present calculation) by less than 1%.

In a further study of band mixing in W^{183}, Rowe[42] sought to determine whether or not $\Delta K=\pm 2$ band mixing was also important. He found that when the $\Delta K=\pm 2$ band mixing was large enough to make significant changes in Kerman's mixing parameters a_i, then there was disagreement with the few values of $B(E2)$ obtained from Coulomb-excitation experiments. The present experiment probably gives further evidence for a lack of $\Delta K=\pm 2$ band mixing, since the wave functions for Rowe's solution 2 lead to spectroscopic factors which are in poor agreement with our measured relative spectroscopic factors.

The set of values of U^2 used in calculating the spectroscopic factors was obtained by a simple pairing calculation. A computer code[43] based on the method of Griffin and Rich[44] was used to solve the BCS equations. The computer finds the value of the Fermi energy λ that satisfies the equation

$$N=\sum_i[1-(\epsilon_i-\lambda)/[(\epsilon_i-\lambda)^2+\Delta^2]^{1/2}], \quad \text{(A6)}$$

where N is the number of particles present, ϵ_i is the single-particle energy, and Δ is the energy-gap parameter. The latter was taken to be 0.62 MeV. The quasiparticle energies E_i are given by $E_i=[(\epsilon_i-\lambda)^2+\Delta^2]^{1/2}$.

The probability U_i^2 that state i is empty is obtained from the equation

$$U_i^2=\tfrac{1}{2}[1+(\epsilon_i-\lambda)/[(\epsilon_i-\lambda)^2+\Delta^2]^{1/2}]. \quad \text{(A7)}$$

Fourteen single-particle states were included in the calculation. Most of the single-particle energies used were those given by the Nilsson model[33] with parameters $\eta=4.2$, $\mu=0.45$, and $\kappa=0.05$. Some single-particle energies were adjusted until the $[510]\frac{1}{2}^-$, $[512]\frac{3}{2}^-$, $[624]\frac{9}{2}^+$ and $[503]\frac{7}{2}^-$ quasiparticle energies agreed fairly well with the experimentally known energies. A unique fit could not be obtained. It was found that the U_i^2 for the $[510]\frac{1}{2}^-$, $[512]\frac{3}{2}^-$, and $[503]\frac{7}{2}^-$ states ranged from 0.65 to 0.82, 0.81 to 0.88, and 0.88 to 0.94, respectively. The best fit gave the values $U_i^2=0.73$, 0.85, and 0.91, respectively, for these three intrinsic states. These values

[38] G. R. Satchler, Ann. Phys. (N. Y.) 3, 275 (1958).
[39] S. Yoshida, Phys. Rev. 123, 2122 (1961).
[40] A. K. Kerman, Kgl. Danske Videnskab. Selskab, Mat. Fys. Medd. 30, 15 (1956).
[41] R. T. Brockmeier, S. Wahlborn, E. J. Seppi, and F. Boehm, Nucl. Phys. 63, 102 (1965).
[42] D. J. Rowe, Nucl. Phys. 61, 1 (1965).
[43] We are indebted to A. Lande for the use of his code.
[44] J. J. Griffin and M. Rich, Phys. Rev. 118, 850 (1963).

were used in the calculation of the spectroscopic factors. This set of values of U^2 agrees substantially with a set calculated by Yoshida[2] for W^{183}. We estimate that the uncertainties in U^2 introduce less than a 10% uncertainty into the large spectroscopic factors.

A series of calculations was made in order to test the sensitivity of the spectroscopic factors to the parameters η, μ, and κ of the Nilsson wave functions. The results of these calculations are shown in Fig. 16. The three parameters were varied one at a time about the point $\delta=0.21$, $\mu=0.45$, $\kappa=0.05$. All of the large spectroscopic factors were found to be relatively insensitive to variations in the parameters except for the spectroscopic factor of the $[512]\frac{3}{2}$ state with $I=\frac{3}{2}$. The smaller spectroscopic factors, particularly the one for the ground-state transition to the $[510]I$ state with $I=\frac{1}{2}$, are much more sensitive to changes in the parameters.

In order to reproduce the sequence of levels in the shell model for zero deformation, Nilsson[32] chose the values $\mu=0.45$ and $\kappa=0.05$ for the $N=5$ oscillator shell. Another set of parameters ($\mu=0.34$ and $\kappa=0.50$) has been proposed for W^{183} by Brockmeier *et al.*[41] These authors, however, chose values for the parameters that reproduced the experimentally observed values for the decoupling parameter a and the energy separation between the $[510]\frac{1}{2}$ and $[512]\frac{3}{2}$ intrinsic states. With this set of parameters, however, the relative energies of shell-model levels for $\delta=0$ are somewhat more poorly reproduced than with Nilsson's original choice of parameters. This might be expected since it is probably unreasonable to ask the Nilsson wave function to give the correct value for the decoupling parameter, a quantity which depends very sensitively on weighted differences between the various values of the C_{jl}. Furthermore, the set of parameters proposed by Brockmeier *et al.* leads to spectroscopic factors which are a poorer fit to our experimental data. In particular, the predicted cross section of the $[512]\frac{3}{2}$ state with $I=\frac{3}{2}$ is almost twice what we observe. Consequently we have used Nilsson's original choice for μ and κ in our calculation of the spectroscopic factors.

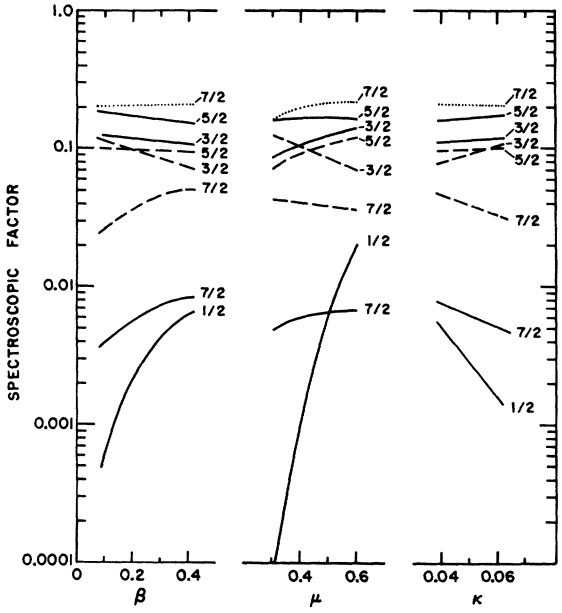

FIG. 16. The theoretical spectroscopic factors for the W^{183}-$(d,p)W^{183}$ reaction, plotted as a function of each of the parameters β, μ, and κ of the Nilsson wave functions. The effects of Coriolis band mixing and the pairing interaction are held constant. Each curve is labeled with the spin I of the final state W^{183}. The three rotational bands $[510]\frac{1}{2}$, $[512]\frac{3}{2}$, and $[503]\frac{7}{2}$ are indicated by solid, dashed, and dotted lines, respectively.

It is difficult to assess the accuracy of the calculated spectroscopic factors. However, some idea of the accuracy can be gained from the uncertainty in the various quantities needed to evaluate Eq. (A5). The uncertainty in the values of C_{jl} is probably the most important source of uncertainty. Judging from the variation in S in response to changes in δ, μ, κ, and U_i^2 a reasonable estimate for the uncertainty in the large spectroscopic factors might be 30%, except that the $[512]\frac{3}{2}$ state with $I=\frac{3}{2}$ would have a somewhat larger uncertainty. The spectroscopic factor for the transition to the $[510]\frac{1}{2}$ state with $I=\frac{1}{2}$ (the ground state), however, is probably known only within about a factor of 2.